International Journal of Hydrogen Energy 49 (2024) 1319–1331

Contents lists available at ScienceDirect

International Journal of Hydrogen Energy

journal homepage: www.elsevier.com/locate/he

Gas composition tracking feasibility using transient finite difference θ-scheme model for binary gas mixtures

Matej Urh [a,b,*], Miloš Pantoš [b]

[a] Plinovodi d.o.o., Cesta Ljubljanske brigade 11b, 1001 Ljubljana, Slovenia
[b] University of Ljubljana, Faculty of Electrical Engineering, Tržaška cesta 25, 1000 Ljubljana, Slovenia

ARTICLE INFO

Keywords:
Model validation
Hydrogen
Transient gas pipeline system model
Binary gas blends
Concentration tracking
Looped network topology

ABSTRACT

Implicit finite difference method is popular numerical method for simulation of transient pipeline dynamics, governed by the system of Euler partial differential equations. If advection equation is included in the mathematical formulation, gas composition tracking is also possible. If implicit scheme is used for gas composition tracking, simulated concentration profiles are distorted due to the occurrence of numerical diffusion, a non-physical phenomenon, caused by the 1st order accurate numerical implicit scheme. Intensity of the numerical diffusion can be decreased by use of θ-scheme with arbitrarily chosen implicitness. In order to evaluate accuracy of such numerical scheme and adequacy for usage in actual application, numerical model must be evaluated on actual gas pipeline system topology with actual measured boundary conditions and compared to actual measured results. Aim of this paper is to assess whether hydrogen concentration tracking is feasible using such approach considering complex grid topologies. Paper highlights the peculiarities of the proposed θ-scheme and finite difference method and its impact on the calculated concentration profile for binary gas mixtures. Non-physical flow reversal issue and its impacts on concentration tracking in looped pipeline system is researched and explained. Simulation results shows high accuracy for simulated values of hydraulic variables compared to the measured values, in some cases fit is perfect. Discrepancy between measured and the simulated values of the pressures at nodes on the main transport route is negligible, while the discrepancy increases with the distance from the main transport routes. The largest discrepancy occurred on the most distant node and was between 1.7006 bar (4.85%) and 1.7119 bar (4.88%), depending on the θ value. On the other hand, simulated concentration profile lacks finer details due to the numerical diffusion effects while the simulated concentration profile lags the measured profile, partly by the impacts of the 1st order accurate scheme and partly by effects of non-physical reversed flows. Discrepancy between simulated and measured amplitude of the tracked concentration profile was negligible, while discrepancy due to the time delay of the simulated and measured profile was more expressed and ranged between 2h to 9h. Largest time delay was caused by the non-physical flow reversal.

1. Introduction

Gas sector has changed significantly in the recent times and will continue to change, mainly due to the climate agreement requirements and the recent geopolitical conflict between Russia and Ukraine which resulted in war. Climate agreements resulted in EU climate packages e.g. Fit for 55, which aims at reduction of the green house gas (GHG) emission for 55% by 2030 compared to GHG levels in 1990 [1]. Ambitious goals of the package Fit for 55 were further increased in the RePowerEU package — measures to decrease imports of natural gas from Russia, reduce use of fossil energy sources and to increase diversification and security of supply as an answer to Russian aggression in Ukraine [2]. To achieve this ambitious goals, gas sector will have to transform significantly. Natural gas consumption will have to be decarbonized, which can be achieved by replacing natural gas with hydrogen, biomethane or synthetic methane. Those gases can replace natural gas completely, or they can be mixed with it, replacing it gradually although certain limitations apply due to the safety and compatibility reasons in case of mixing (blending) [3,4]. While biomethane and synthetic methane are very similar to the natural gas (main component of them being methane), hydrogen, on the other hand, is very different from the methane based gases. Hydrogen thermodynamic properties differs significantly, for example volumetric calorific value (GCV) of the hydrogen is only one third of the GCV of natural gas (gross calorific value (GCV), also known as high heating value (HHV)

* Corresponding author at: University of Ljubljana, Faculty of Electrical Engineering, Tržaška cesta 25, 1000 Ljubljana, Slovenia.
E-mail addresses: matej.urh@plinovodi.si (M. Urh), milos.pantos@fe.uni-lj.si (M. Pantoš).

https://doi.org/10.1016/j.ijhydene.2023.11.031
Received 22 August 2023; Received in revised form 28 October 2023; Accepted 2 November 2023
Available online 7 November 2023

is commonly used by the EU gas system operators and in the EU gas sector to indicate energy content of the gas). From that reason the transmission capacity of the hydrogen pipeline system is reduced compared to the natural gas system [5,6], although such capacity reduction can be mitigated to a limited extent by e.g. increasing the gas flow velocity [7].

Research of this paper highlights topic related to natural gas — hydrogen blending approach to decarbonization of natural gas use. Other aspects of hydrogen value chain e.g. production [8,9], storage [10,11] and application [12] along with the environmental and economic assessment [13,14] are out of the scope of this research and can be found in available literature.

From the reasons explained above, new approaches to the gas system operation and planning are required by the gas transmission system operators (TSO). Introduction of renewable hydrogen to the gas system requires dynamic modeling to capture all phenomena caused by hydrogen injection, steady-state models are unable to properly address that phenomena [15]. Renewable hydrogen can be produced from either biological processes [16] or renewable electricity [17], primarily from the photovoltaics (PV) and wind, which are intermittent sources. Since majority of the renewable electricity will be consumed in power system, only renewable electricity surpluses will be used for hydrogen production [18,19]. That way hydrogen production will be affected by both RES production and electricity load consumption uncertainties [20–22], which will result in a dynamic hydrogen production and gas grid injection. Hydrogen blended with natural gas causes local variations of the GCV, density, compressibility and other thermodynamic properties which affects the line pack of the system, pressure levels and flow dynamics of a larger part of the system [5,23].

Implicit finite difference method is a popular method for modeling transient gas pipeline hydraulics and gas composition tracking, although it is not perfect, its main drawback being numerical diffusion caused by 1st order accurate implicit numerical scheme. There are multiple approaches to reduce impacts of numerical diffusion for example utilization of higher order numerical schemes [24,25]. Effects of numerical diffusion can also be reduced by implementation of θ-scheme, where implicitness of the scheme can be arbitrarily defined by changing the value of the θ parameter. If $\theta = 1$, the scheme is 1st order implicit scheme, if $\theta = 0.5$, the scheme is 2nd order Crank–Nicolson scheme. While implicit scheme causes numerical diffusion, Crank–Nicolson scheme causes spurious oscillation, so they are not the best choice [26]. That is why we seek better tradeoff between the two numerical phenomena in schemes with $0.5 < \theta < 1$. If $\theta = 0$ the scheme is 1st order explicit scheme, which is subjected to the CFL condition [27] and therefore limited to small temporal and spatial discretization steps. From that reason authors avoid schemes with $0 < \theta < 0.5$. This paper focus on the validation of the θ-scheme on actual network topology using actual measured boundary conditions. This paper is the first to offer results of θ-scheme model validation. For comparison, concentration tracking results obtained by implicit scheme model are also included in this paper.

Papers which address validation of pressure and flow calculations using actual network topology and real operational data are available [28,29]. Dynamic models of the gas system utilizing implicit finite difference method which also enables to address impacts of variable hydrogen injection are available [15,30–36], yet not many of them are properly validated.

For example model in [30] is validated using non-realistic gas system topologies. On the other hand, the same topologies, although non-realistic, are used in more than just one paper and from that reason are useful to compare accuracy and performance of different modeling and simulation methods and approaches. Example of such benchmarking of hydraulic variables such as pressure and flow is a simple triangular network with three nodes and three pipelines. This network topology is used in [30,37–42] and enable comparison of many different methods and modeling approaches. Unfortunately this benchmarking network topology is not used for hydrogen tracking in the literature. For example paper [30] proposes method to track propagation of hydrogen effects in the gas system based on calorific value tracking, called calorific-value-gradient method. Accuracy of pressure and flow simulation is benchmarked using the triangular network while hydrogen tracking is tested on the adapted triangular network. Since adapted triangular network is not used for benchmarking purposes in the literature, accuracy of the proposed method cannot be compared to other methods although paper compares the accuracy of calorific-value-gradient method and implicit finite difference method.

Paper [15] study hydrogen tracking in case of multiple hydrogen injections. Model is solved by the implicit finite difference method with Soave-Redlich-Kwong EoS. Although paper uses actual 20-node Belgian transmission system to validate accuracy of the proposed model, measurement and operational data for actual operation with hydrogen are not available. In that case calculated hydrogen concentration profiles cannot be benchmarked against actual measurements. Actual measured gas flow is also different from simulated gas flow.

Some papers, for example [32] are validated using actual system topologies and operational data. Results of such model validation are more valuable to the engineers and system operators as they offer more detailed insight into the realistic operating conditions and the phenomena associated with them.

Paper [32] uses actual measurements to validate the accuracy of the proposed hydrogen concentration tracking model. Paper compares the accuracy of the Eulerian frame of reference based implicit finite difference method and Langrangian frame of reference based batch tracking method. Method uses GERG-2004 equation of state (EoS). Accuracy of both methods is validated on two cases: onshore pipeline connecting underground gas storage (UGS) of Polish transmission system and an offshore single pipeline of the Norwegian gas export system. Since hydrogen is not yet present in the simulated pipelines, ethane concentration tracking is used to validate the model, similarly as in our paper. In both cases model was validated on a single pipeline model with no loops. The same pipeline of the Polish transmission system is also used for model validation in [31].

Authors in [34] test concentration tracking of multiple gas components on an actual part of the Spanish gas system. System topology used for the model validation is more complex compared to [31,32] since it consists more than just a single pipeline. Paper proposes uncoupled approach to solve flow and advection equations separately, applying different mesh size and different numerical equation to each set of equations. Model does not implement implicit theta scheme and therefore validation results do not give any insight into the accuracy and performance of the implicit finite difference method and consequently are not appropriate to assume accuracy of the θ-method. The same gas system topology was used in [35] where finite volume method was used for simulation. Similar topology complexity was also used for validation purposes in [33] but also in this paper authors used finite volume method to simulate gas components concentration tracking.

Based on the available literature we conclude there are no papers available on validation of 1st order finite difference method (implicit or θ-scheme) on actual network with complex topology (branched and looped networks) and with measured data, which are used both as a boundary conditions in the simulation and as a reference for simulation results validation. The main motivation for this paper is

therefore to validate θ-scheme finite difference method, which is similar to the implicit finite difference method, using measured data and real network topology. Our paper proposes simplified approach to the hydrogen concentration tracking, by assuming natural gas — hydrogen blend is binary mixture instead of simulating multiple gas components. Complexity of the numerical model is reduced if binary mixture is assumed. Results of our paper offer insights on the method accuracy in real network topology and operating scenarios and can help engineers and operators decide whether θ-scheme method and binary mixture assumption suits the needs of their simulation requirements. Our paper also addresses impact of non-physical flow reversal on gas species concentration tracking. Non-physical flow reversal can occur in looped network topologies and its impact on accuracy of concentration tracking is also not addressed in available literature. The main objectives ot this study are:

1. to investigate if the θ scheme for the binary mixtures is appropriate from the accuracy and complexity point of view for actual application in the gas hydraulic simulation related tasks used by the system operators
2. to investigate performance of the scheme with finite difference method in case of complex gas system topologies based on the actual gas systems.

Novelty of this paper is the investigation of the simplified approach to the concentration tracking assuming binary gas mixture, which leads to the reduced mathematical complexity of the model. Proposes simplified approach was validated on the actual complex gas system topology using actual measured data.

This paper is organized as follows. In Section 2 mathematical model and its simplifications are presented and explained. Final form of the discretized model equations are included in Appendix. Topology of the actual gas system, part of the Slovenian gas transmission system, used for the model validation purposes is described in Section 3. Available operational data used as an input and other input data calculated using operational data are also explained in the Section 3. Validation of the simulation results and comparison with the actual measurements is in Section 4. Final remarks with suggestions for improving the accuracy of the model using more measured data are in Section 5.

2. Mathematical model

Mathematical model is based on the system of non-linear hyperbolic equations, consisting of system of Euler equations which governs hydraulics and mass transfer equation, also called advection–diffusion equation. Those equations are presented and explained in [15,23,28–45]. Model in this paper is simplified, assuming the following assumptions:

1. natural gas is assumed as a single gas mixture component and natural gas — hydrogen blend is a binary mixture
2. low gas velocities, which are significantly lower than the speed of sound in the gas mixture
3. constant elevation of the gas system
4. constant gas temperature and negligible temperature variations throughout the gas system due to ground laid pipelines
5. negligible diffusion mass transfer mechanism
6. negligible radial direction changes compared to the axial direction changes of the simulation variables
7. pipeline junctions have no volume
8. all input gas flows are mixed perfectly in junction meaning all output gas flows have the same gas composition

Based on those assumptions, 1-dimensional isothermal model can be used for the simulation of pipeline hydraulics and gas species concentration tracking:

$$\frac{\partial \rho}{\partial t} + \frac{\partial (\rho v)}{\partial x} = 0 \tag{1}$$

$$\frac{\partial (\rho v)}{\partial t} + \frac{\partial \left(\rho v^2\right)}{\partial x} + \frac{\partial p}{\partial x} + \frac{f \rho v |v|}{2D} + \rho g \sin \alpha = 0 \tag{2}$$

$$\frac{\partial y_i}{\partial t} + v \frac{\partial y_i}{\partial x} + D_{diff} \frac{\partial^2 y}{\partial x^2} - R_{reac} = 0 \tag{3}$$

where ρ, v, p, f, D, g, α and y_i are respectively the gas density, the flow velocity, the gas pressure, the Darcy friction factor, the pipeline diameter, the gravity acceleration, inclination of the pipeline and the molar fraction (concentration) of the gas species i. Variables D_{diff} and R_{reac} are diffusion coefficient and rate of chemical reaction in the mass flow, but are omitted in our mathematical model since diffusion is negligible mechanism in case of transmission gas pipeline flows and also no chemical reactions are occurring during the gas transport. Eq. (1) is mass conservation or continuity equation, Eq. (2) is momentum conservation equation or Newton's second law of motion and Eq. (3) is advection equation which governs mass transfer of a gas species in gas mixture. To calculate friction factor Schifrinson equation [46] was used:

$$f = 0.11 \left(\frac{k}{D}\right)^{\frac{1}{4}} \tag{4}$$

Variables ρ and v in Eqs. (1)–(3) are not available through measurements on the gas system. Variable ρ is replaced by mass flow $\dot{m}$, velocity v is expressed with mass flow $\dot{m}$ by introducing mass flow equation and equation of state.

$$\dot{m} = \rho v A \tag{5}$$

$$\frac{p}{\rho} = \frac{Z R T_{amb}}{M} \tag{6}$$

where A, Z, R and M are respectively cross-sectional area of the pipeline, compressibility factor, gas constant and molar mass of the gas mixture. Mass flow could be also replaced by volumetric flow or energy flow, but this model utilizes mass flow, which is also necessary to define conditions in the pipeline junctions. Molar mass of the gas mixture is defined by molar fraction of each gas species in the mix:

$$M = \sum_{i=1}^{N} y_i M_i = y \left(M_{H2} - M_{NG}\right) + M_{NG} \tag{7}$$

where y is a molar fraction of a hydrogen.

Equation of state Eq. (6) introduces gas compressibility Z, which ca be defined by different equations, for example GERG 2008, Papay, Soave-Redlich-Kwong, Benedict-Webb-Rubin, etc [37,45]. This paper utilizes AGA88 equation [23,46]:

$$Z\,(p,T) = 1 + 0.257 \frac{p}{p_c} - 0.533 \frac{p T_c}{p_c T} \tag{8}$$

where p_c and T_c are critical pressure and temperature of the gas mixture and are can be expressed by molar concentration of each gas species.

$$p_c = \sum_{i=1}^{N} y_i p_{c,i} = y \left(p_{c,H2} - p_{cNG}\right) + p_{c,NG} \tag{9}$$

$$T_c = \sum_{i=1}^{N} y_i T_{c,i} = y \left(T_{c,H2} - T_{cNG}\right) + T_{c,NG} \tag{10}$$

Pipeline system with more than one pipeline contains pipeline junctions. Two additional equations are necessary to describe pipeline junction conditions. Pipeline junction hydraulics are defined by mass continuity equation (11).

$$\sum_{i=1}^{N_{in}} \dot{m}_{in,i}^{n+1} - \sum_{i=1}^{N_{out}} \dot{m}_{out,i}^{n+1} + \dot{m}_{injection}^{n+1} - \dot{m}_{offtake}^{n+1} = 0 \tag{11}$$

Gas mixture composition of the junction output gas flows is proportional to the mass fraction Y of a gas species i of input components, meaning mass concentration of the species of input flows must be known. Since molar mass is the unknown variable in this model, mass concentration in expressed by molar concentration by Eq. (12). Assuming binary gas mixture, junction mixing is defined by Eq. (13).

$$Y_i = y_i \frac{M_i}{M} \tag{12}$$

$$\sum_{i=1}^{N_{in}} \frac{y_{in,i}^{n+1} M_{H2} \dot{m}_{in,i}^{n+1}}{y_{in,i}^{n+1}\left(M_{H2}-M_{NG}\right)+M_{NG}} + \frac{y_{injection}^{n+1} M_{H2} \dot{m}_{injection}^{n+1}}{y_{injection}^{n+1}\left(M_{H2}-M_{NG}\right)+M_{NG}} - \frac{y_{out}^{n+1} M_{H2}}{y_{out}^{n+1}\left(M_{H2}-M_{NG}\right)+M_{NG}} \sum_{i=1}^{N_{in}} \dot{m}_{in,i}^{n+1} = 0 \tag{13}$$

Pipeline system also consists of gas compressors. In this paper, gas compressor model is very simplified. It is modeled as a stationary element, with no transients due to the compressor start and ramping up to suitable operational point. In this simplified model compressor is modeled as a node with known pressure ratio:

$$r = \frac{p_{out}}{p_{in}} \tag{14}$$

where r is the compression ratio. In case r > 1, node represent the compressor, in case r < 1 node represents pressure reduction.

Consumption of the gas consumers is defined by their energy demand and since calorific value of the gas mixture is variable, consumption cannot be expressed in volumetric units, but in energy units. Since our model operates with mass flows, not energy flows, known energy offtake must be converted to mass flow with gas composition (binary mixture in our case) taken into account. Offtake is converted from energy to mass flow using Eq. (15).

$$\dot{m}_i^{n+1} = \frac{E}{3600\left(\frac{y_i^{n+1} M_{H2}}{y_i^{n+1}\left(M_{H2}-M_{NG}\right)+M_{NG}}\left(H_{H2}-H_{NG}\right)+H_{NG}\right)} \tag{15}$$

Considering Eqs. (1)–(3) and (6)–(10), simplified transient gas pipeline model for concentration tracking of binary gas mixtures is defined by pipeline Eqs. (16)–(21), nodal Eqs. (11) and (13), compressor/pressure reduction Eq. (14) and offtake Eq. (15).

$$\frac{\partial p}{\partial t} + \frac{K_1 Z}{y\left(M_{H2}-M_{NG}\right)+M_{NG}} \frac{\partial \dot{m}}{\partial x} = 0 \tag{16}$$

$$\frac{1}{A}\frac{\partial \dot{m}}{\partial t} + \frac{\partial p}{\partial x} + \frac{K_2 \dot{m}\,|\dot{m}|}{y\left(M_{H2}-M_{NG}\right)+M_{NG}} = 0 \tag{17}$$

$$\frac{\partial y}{\partial t} + \frac{K_1 \dot{m}}{p\left(y\left(M_{H2}-M_{NG}\right)+M_{NG}\right)} \frac{\partial y}{\partial x} = 0 \tag{18}$$

$$Z\left(y,p,T=const\right) = 1 + \frac{p}{y\left(p_{c,H2}-p_{c,NG}\right)+p_{c,NG}} \left(0.257 - 0.533\frac{y\left(T_{c,H2}-T_{c,NG}\right)+T_{c,NG}}{T}\right) \tag{19}$$

$$K_1 = \frac{RT}{A} \tag{20}$$

$$K_2 = \frac{RTf}{2A^2 D} \tag{21}$$

This model can be used to simulate multiple hydrogen injections in various nodes throughout the system.

2.1. Discretization

Pipeline elements of the gas system are discretized — divided into non-physical nodes which are Δx apart from each other. Discretized version of Eqs. (16)–(18) are applied to each of the non-physical node, except to the first node of each pipeline element. Pipeline Eqs. (16)–(18) are discretized using two forms of the θ-scheme: centered θ-scheme (22) and left sided θ-scheme (23).

$$\frac{\partial r}{\partial x} = \frac{1}{2\Delta x}\left(\left(1-\theta\right)\left(r_{i+1}^{n} - r_{i-1}^{n}\right) + \theta\left(r_{i+1}^{n+1} - r_{i-1}^{n+1}\right)\right) \tag{22}$$

$$\frac{\partial r}{\partial x} = \frac{1}{2\Delta x}\left(\left(1-\theta\right)\left(3r_i^n - 4r_{i-1}^n + r_{i-2}^n\right) + \theta\left(3r_i^{n+1} - 4r_{i-1}^{n+1} + r_{i-2}^{n+1}\right)\right) \tag{23}$$

θ-scheme is the convex linear combination ot the implicit and explicit Euler schemes and is actually a family of schemes with different implicitness. Level of implicitness is defined by an arbitrarily chosen parameter $\theta \in [0,1]$. If $\theta = 0$ the scheme is fully explicit, in case $\theta = 1$ scheme is fully implicit and if $\theta = 0.5$ the scheme is Crank–Nicolson or trapezoidal. Scheme is absolute stable for $\theta \in [0.5,1]$. For $\theta = 0.5$ the scheme is second order accurate while for $\theta \neq 0.5$ the scheme is first order accurate [47,48].

Discretized pipeline system consists of many physical and non-physical nodes, each with its own input and output options and different sets of equations applied to them. All nodes used in the model are listed and described in the Table 1. Physical pipeline is defined with two physical nodes, input node and output node. If the pipeline input is not connected to pipeline junction, e.g. input pipeline in the gas system from the gas source or the IP, type A or type B applies. If pipeline output is not connected to the pipeline junction, e.g. offtake at the end of the pipeline branch, type C or type D applies. Input and output nodes of multiple pipelines can be joined into the pipeline junction. Pipeline junction dynamics are defined by Eqs. (11), (13) and (14). Those equations are not discretized, since they represent element that has no volume and no length. In our model physical junction consist of physical input (type E) and physical output (type F) nodes of the pipelines joined in the junction. Similarly physical compressor or pressure reduction node is defined by Eq. (14) and it consists of compressor/pressure reduction input node (type G) and output node (type H). Discretization of the pipeline creates majority of the model nodes - non-physical nodes of type I.

For each node of the discretized model, multiple equations apply, except for the pipeline inputs, which are not directly included into the numerical formulation, since variables for the first (input) node in a pipeline (node types A,B,E,G) are already included in the equations of the downstream nodes. Equations applied to the nodes according to Table 1 form system of non linear equations, which must be solved numerically. In this paper Newton–Raphson method [49] is used to solve the system of nonlinear equations.

3. Gas transmission pipeline system model

Topology of the gas pipeline transmission system model used for validation of the transient binary gas mixture hydraulic and concentration tracking model is slightly simplified part of the actual gas transmission system topology. All input data are actual measurements of flow, pressure and gas composition, obtained from the main SCADA system of the gas TSO. Flow and pressure measurements are available for all offtake nodes, while gas composition measurements are available only on the interconnection points (IP).

Numerical model of the gas pipeline system consists of 9 different types of nodes, described in Section 2.1. Purposes of nodes like junction and compressor/reduction nodes is straightforward while input and offtake nodes can be both flow or pressure type of node and they must be selected carefully since the type of the selected node can affect simulation results significantly. All types of nodes are defined in Table 1.

Table 1
Model node types.

Node type	Description	Known variables	Unknown variables	Physical node	Applied equations	Input nodes	Output nodes
A	Pressure input	p, y	$\dot{m}$	Yes	/	/	I
B	Flow input	E, y	$\dot{m}$, p	Yes	/	/	I
C	Pressure output	p	$\dot{m}$, y	Yes	(28), (29), (30)	I	/
D	Flow output	E	$\dot{m}$, y, p	Yes	(15), (28), (29), (30)	I	/
E	Pipeline junction input	$\dot{m}_{injection}$, $y_{injection}$, $\dot{m}_{offtake}$	$\dot{m}$, y, p	Yes	/	I	F
F	Pipeline junction output	$\dot{m}_{injection}$, $y_{injection}$, $\dot{m}_{offtake}$	$\dot{m}$, y, p	Yes	(11), (13), (28), (29), (30), (15)	E	I
G	Compressor input/ pressure reduction input	r	$\dot{m}$, y, p	Yes	/	I	H
H	Compressor output/ pressure reduction output	r	$\dot{m}$, y, p	Yes	(14), (28), (29), (30)	G	I
I	Discretized nodes	/	$\dot{m}$, y, p	No	(25), (26), (27)	A,B,F,H	C,D,E,G

When building the gas transmission pipeline system model uncertainties of input data, model uncertainties and numerical uncertainties were considered [50]. Uncertainty regarding input data originates mostly from the different timescales of measurements of various quantities, which are described more detailed in Section 3.1, and from topology simplifications which are explained more detailed in Section 3.2. Model uncertainty was addressed by applying different θ parameters to the simulation while different types of models were not considered in this paper, since the focus of this paper is θ-scheme finite difference model with binary gas mixtures. Numerical uncertainty, which steam from the truncation error of the Taylor series representation of the derivatives was studied through basic model parameter variations — spatial discretization step and simulation timestep. Both spatial discretization steps and temporal discretization step were selected based on optimal accuracy to the computational cost ratio.

3.1. Input data

Measurements of flows, pressures and gas composition are available in different time resolution. IP quantities are usually measured in finer time resolution than other quantities on the transmission system. Data samplings of measurements of all quantities are defined by constant time resolution (scan rate) and by rate-of-change, meaning if the measured quantity changes more than defined percentage of the sensor measurement range, quantity value is measured and stored, regardless of the preset scan rate. That way TSO have more detailed data in case of rapid changes of the measured quantity. Constant time resolution for measurements on IPs are usually set to 2 min, while measurement of quantities on offtake points throughout the system are usually set to higher scan rates of up to 1 h. For majority of the measurements used in this paper, finer time resolution of data is available in some time periods due to the rate-of-change settings.

Since data measurements required for the simulation are of different time resolution and not synchronized with each other, linear interpolation was utilized to calculate, if not available, values for all inputs in 1 min time resolution, starting with the same time. That way input data was synchronized and prepared to be used in simulation with various simulation time steps.

Natural gas is a mixture of many gases. It consists primarily of methane (≈95%mol) and other hydrocarbon gases such as ethane (≈3%mol), butane, propane, pentane and their isomers, etc. Inert gases such as nitrogen and carbon dioxide are also present. Since numerical model considers binary gas mixtures, mixture of natural gas without ethane and ethane as a separate gas are considered for model validation purposes. Composition of natural gas varies with time due to variations of concentration of all natural gas components, not only ethane, as it is assumed in our simulation. Thermodynamic input data, such as M, H, p_C and T_C for natural gas component of the gas mixture are calculated based on the measured data from the gas chromatograph located on the input IP. Thermodynamic quantities M, p_C and T_C of a gas mixture were calculated using Eqs. (7), (9) and (10), respectively. To calculate GCV in kWh/kg units, required for the simulation, molar fractions were first converted to mass fractions using Eq. (12), then GCV of gas mixture was calculated using:

$$H = \sum_{i=1}^{N} Y_i H_i \tag{24}$$

Table 2
Values of thermodynamic properties for gas mixture without ethane used for the simulation.

Thermodynamic property	Unit	Natural gas	Ethane
M	g/mol	16.615	30.07
H	kWh/kg	15.351	14.147
p_C	bar	46.539	48.820
T_C	K	192.642	305.32

Time series of the natural gas component of the gas mix are in Fig. 1. Since our model supports only concentration tracking of two gas components with constant thermodynamic properties, average values for the thermodynamic quantities for natural gas component of the mix are assumed.

With this assumption accuracy of the results is decreased, but not significantly since the variability of the time series of other natural gas components is relatively small. Thermodynamic properties are in Table 2. Since proposed model is isothermal, constant gas temperature of 283.15 K was assumed for the simulation. Use of isothermal model results in less accurate results, impacts of isothermal model on the accuracy is explained in [44].

Offtake measurements are available in volumetric units (Nm^3/h). Model requires offtakes in energy units (kWh/h) and since distribution of GCV of the natural gas throughout the system at time $t = 0$ and measurements of GCV at offtake nodes are not available, GCV measured at node 1 is assumed to be equal in all nodes at time $t = 0$ and time series of GCV variations, measured at the node 1 are assumed to be equal for all offtake nodes for calculation of the energy offtakes from measured volumetric offtakes. With this assumption, changes of GCV in node 1 are instantly (in the same time step) applied in all nodes of the gas system, which decreases accuracy of the model.

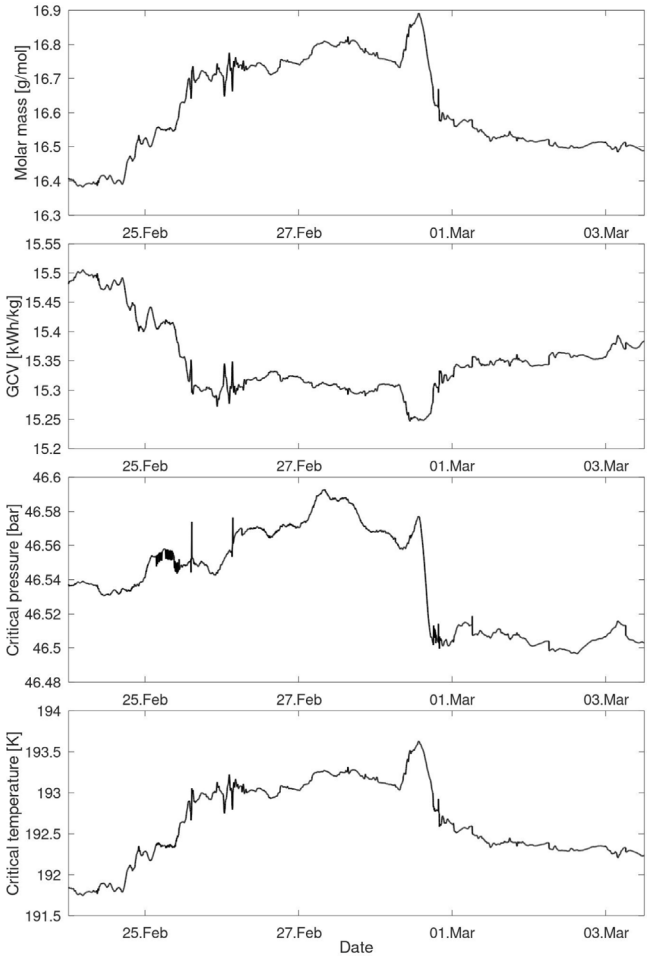

Fig. 1. From gas composition measurements calculated changes in molar mass, GCV, critical pressure and critical temperature of the gas mixture without ethane.

Flow measurements are available for all offtake and input nodes, while pressure measurements are not available for all offtake nodes (or pressure measurements after pressure reduction at the offtake nodes are available, but are not suited for the model), but based on experience gained during building the real case model, only one pressure node (at least one pressure node is required in the model, to define pressure levels) is implemented in the model. In the simulated scenario flow direction in the subsections of the pipeline section between nodes 9 and 16 changes direction multiple times during the simulation period. In reality, flow did not changed the direction in actual operation during the simulated period. Since pressure differences on the certain parts of the system can be very small, pressure measurements in offtake nodes can be very close to those calculated pressures in non-physical nodes upstream of the offtake nodes, which could lead to significantly distorted offtake flow calculations. If calculated pressures in nodes upstream of the offtake nodes are lower than offtake pressures due to the accuracy errors, flow direction can even be reversed and offtake node can become injection node, which distorts hydraulics of the system significantly. From that reason all offtake nodes are modeled with flows.

3.2. Transmission system model topology

Transmission gas system, used for validation of the numerical pipeline model is a part of the actual Slovenian natural gas transmission system. Only pipelines, necessary to adequately track ethane profile are used in the model, meaning only pipelines which connects input IP chromatograph with output IP chromatograph. Along this main transmission route, designated with thick lines in Fig. 3, offtake branches, designated with thin lines in Fig. 3 are modeled where distance from the main transmission pipeline route to the offtake point is too distant and would cause deviations of simulated results compared to the measurements due to time delay of the actual offtake profiles caused by the distance. This paper considers offtake points which are located less than 2 km away from the main pipeline as offtakes on the main pipeline (e.g. node 2), while offtake points located more than 2 km are considered as a separate branch from the main pipeline (e.g. node 24).

More complex branches, e.g. branches originating form nodes 3, 16 and 12 are necessary because of their distance from the main pipeline and large offtakes at the end of those branches. If all the offtake of the branch is considered in one single node, simulation results would be less accurate. For example offtake at node 33 which occurs at time t is manifested at node 16 at time $t - \Delta t$. If offtake profile at node 33 and all other offtake profiles on the branch originating in node 16 are just summed and assumed to be located at node 16, actual flow profile at node 16 is distorted significantly. Since flow measurement in node 16 is not available, offtakes on that branch are modeled more detailed — as a separate branch. On the other hand, from node 2 whole pipeline with multiple offtake points and multiple branches originates, but since flow measurement in node 2 is available, modeling of that pipeline as a separate branch is not necessary for the simulation scenario. Greater availability of the measurements of flow and pressure on the various nodes in the pipeline system leads to less complex topology and reduced numerical complexity of the model.

Time delays for the offtake profiles are caused by the compressibility of the gas and the length of the pipeline connecting the remote offtake node and the main pipeline. Longer pipelines leads to more elastic behavior of the systems hydraulics meaning higher time delays between occurrence of hydraulic features (feature on pressure or flow profile) at the end and at the beginning of the pipeline. If branch pipeline lengths are small, flow profiles of offtake points, distributed on a branch could be summed up and considered as if sum of the flows occurs in the offtake node on the main pipeline. On the other hand, if the branch lengths are large, such approach is not suitable since it introduces non-negligible errors in simulation results. Compressibility of the gas in the system can cause amplitudes of the flow profile on the node on the main pipeline where the branch originates, to be higher or lower than amplitudes of the flow profiles of the offtake nodes. Reason for that are the pressures changes throughout the system, which can cause pressure waves which causes flow profiles which can be higher or lower than corresponding offtakes.

In case long branches are neglected and all offtakes are summed and considered as an offtake on the main pipeline, not only local branch hydraulics can be affected, but hydraulics on the wider system area or, if the branches are long enough and pressure variations throughout the system high enough, hydraulics of the whole system. Effects of both the time delays of flow profiles due to the branch pipeline length and of the gas compressibility and pressure variations are simulated on Fig. 2. Simulated flow profile in node 16 is compared to the sum of measured offtake flows on all branch nodes (nodes 27 to 33).

Part of the gas system, used for model validation, also has two pressure reduction nodes, nodes 5 and 40. For both nodes input and output regulator pressures measurements are available and they are modeled as a nodes with known pressure ratio. Pipeline lengths and diameters are presented in Fig. 3.

Since exact pipeline roughness for each pipeline is not available, roughness of 13 μm was assumed. For this simulation spatial discretization step $\Delta x = 1000$ m was used. In case smaller spatial discretization step Δx is used, model is more accurate but computational time increase significantly. The discretized model consists of 506 nodes. Discretized pipeline must contain at least three (physical and non-physical) nodes because of the three node stencil used in the implemented numerical scheme.

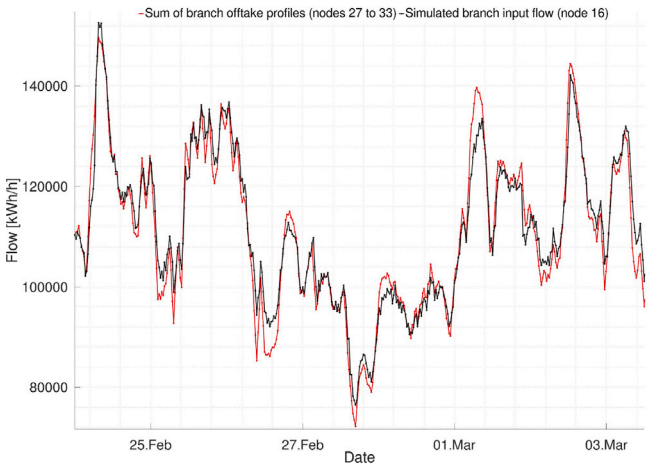

Fig. 2. Comparison of sum of all measured offtakes in nodes 27–33 and simulated flow in the branch 16–27 at $\theta = 0.8$.

3.3. Simulation scenario

Model is validated on an actual operational case, based on measurements in span of 7 days, taken in February 2022. Simulation scenario simulates traveling of impulse of ethane, measured on transmission system entry IP with Austria (node 1), towards the transmission system exit IP with Croatia (node 23). Measurements of the ethane impulse on the entry and exit nodes are shown in Fig. 7.

Gas mixture flows from the input node 1 towards the exit node 23 via two routes: longer route 1-4-5-16-23, and shorter route 1-4-40-16-23. Due to the offtake dynamics in the section 9–16, pressure levels in that section are very close leading to multiple non-physical flow reversals on the subsections of the section 9–16. SAlthough measurements for all physical nodes on the section 9–16 are not available, it is evident that the flow is not reversing on the section 13–16 from the measured pressure difference as can be seen in Fig. 6. Measured flow difference between nodes 13 and 16 is always greater than zero meaning pressure in node 13 is greater than pressure in node 16 during the whole simulation period, therefore flow from node 16 to node 13 is not possible.

If calculated flow values are not negative in all of the non-physical nodes between the two physical nodes, flow is not yet reversed. This is not a problem from the convergence perspective, since a couple of time steps with negative flow values are not problematic and do not cause convergence instability, although the mathematical model assumes constant flow directions. In that case flow values in the partly reversed branch will either change back to positive values, or all the remaining positive flow nodes in the branch will change to negative values. Partial reversal of the flow in a branch is not possible, because in that case one non-physical node will have two input and no outputs or two outputs with no inputs, and such topology configuration is not solvable, as flow direction is implemented in the topology itself. For that reason virtual non-physical branches are introduced into the model, such as branches 9–47 and 13–48 which are implemented purely from numerical stability reasons. If the offtakes in the nodes 47 and 48 are assumed to be on the main pipeline route, in the nodes 9 and 13, respectively, model is not stable. In that case, both nodes could come into the state where they will have two inputs and no outputs. Virtual branches are modeled as a 10 m long with $\Delta x = 5$ m regardless of the Δx used for physical pipelines. In that case the 3 node pipeline requirement is satisfied.

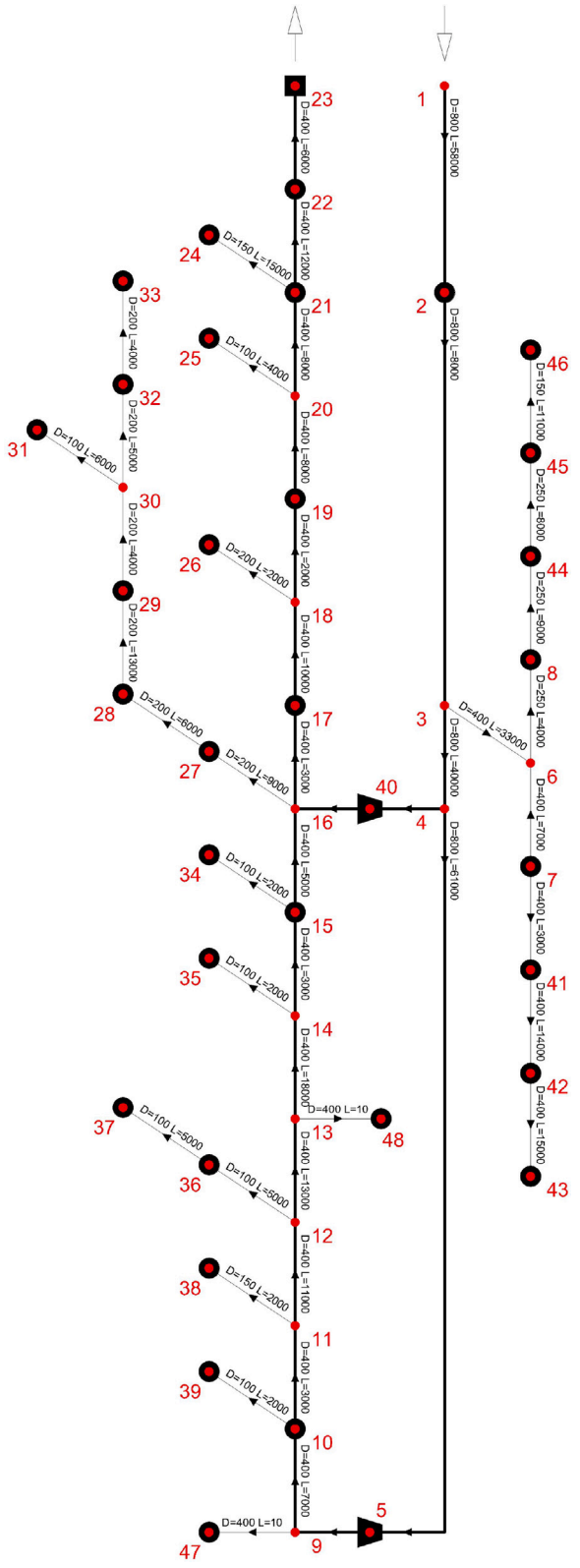

Fig. 3. Topology of simplified transmission system used for model validation.

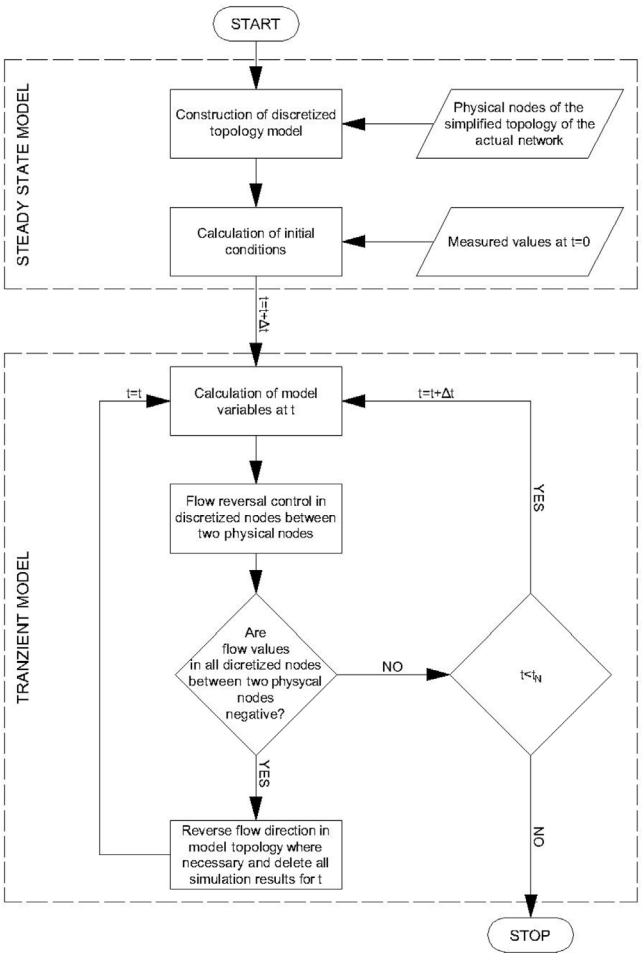

Fig. 4. Model flowchart.

Flow reversal is implemented in the model algorithm but is not a part of the mathematical formulation of the model. Governing equations do not support flow reversal. Reverse flows appears as a negative calculated flow and negative sign causes convergence problem of the mass transfer equation, leading to the non-physical solutions after a couple of the time steps with negative flow values. Algorithm checks if the flows in all non physical nodes (type I) in between the two physical nodes (types A-H) are negative. If they are all negative, flow direction is changed on the topology level of the model, meaning all inputs and outputs of the non-physical type I nodes are simply changed as well as node types E and F and their inputs and outputs where necessary.

Model algorithm flow chart is presented in Fig. 4. Before the calculations starts, algorithm prepares gas system topology based on the physical nodes topology and spatial discretization as an input. Using steady state model, initial conditions for all model nodes are calculated next based on the measured values at t = 0. When initial conditions are calculated, algorithm uses transient model to calculate values for $\dot{m}$, p and y for all physical and non-physical nodes of the model for t = t + Δt. After values for the next time step are calculated, algorithm checks if the flow in any of the branches is reversed — meaning in all non-physical nodes between the two physical nodes. If that is true, topology is changed accordingly and calculation for current time step is repeated, otherwise simulation continues to the next time step. It is possible that flow direction between two physical nodes keeps changing regardless of changes of topology. For that reason number of changes of flow direction for each branch (limited with two physical nodes) in the same time step is limited. In that case flow direction will get into more stable state in the next time steps.

4. Validation

To reduce the complexity of the model, some simplifications of the otherwise known pipeline system topology were implemented and certain assumption to prepare input data were considered, which both lead to the reduced accuracy of the model. Those assumptions and simplifications are:

1. constant composition of the gas without the ethane and consequently constant GCV and molar mass of the natural gas component of the binary mixture
2. simplified network topology
3. different time resolution of the measurements of the input data (some of the up to 1 h)
4. GCV measured at the node 1 is used to determine offtakes in energy units for all offtake nodes
5. non-physical reversal of flow in parts of the system
6. use of 1st order numerical scheme
7. equal pipeline roughness for all pipelines

Assumptions and simplifications are ordered from those with the higher impact on the accuracy to those of the lowest. Ordering is based on the experience of the authors and is not necessarily correct as not all assumptions and simplifications can be assessed separately from each other.

Model is validated by comparing two kinds of results, namely ethane concentration tracking results and pressure values in selected nodes where pressure measurements are available. As can be seen in Figs. 7 and 8, discrepancy between the simulated and measured node pressure in the beginning of the simulation period is high, for some nodes it is actually the highest. It should be noted that this discrepancy has no physical background and it occurs simply due to the fact that the actual gas composition in all the physical and non-physical nodes, except for the nodes 1 and 24, at the beginning of the simulation period (t = 0) is not known. Input thermodynamic properties, presented in Table 2, although reasonably correct for the majority of the simulation period regardless of all the simplifications, are not the same as the properties of the gas mix throughout the system at the time t = 0. From that reason the energy offtakes of the nodes throughout the system calculated using too simplified input data results in inaccurate solution. After a couple of hours in the simulation, when the gas form the input at the time t = 0 reaches all offtake nodes in the system, accuracy of calculated values increases.

Due to small measured pressure difference between the nodes 9 and 16, calculated flow direction reverses multiple times on that pipeline system section due to simulation accuracy errors. Since pressure difference between the both ends of this section is very small, calculation errors have large impact on the calculated flow directions not only in this section but also in the subsections, limited with physical nodes in that section. Calculated flow reversal occurrences on the subsection of the section 9–16 are presented in Fig. 5. Flow reversed multiple times during the simulation period in the various subsections of the section 9–16.

Numerical errors in pressure calculations have caused non-physical flow direction reversals which impacts the accuracy of the ethane concentration tracking results. Actual physical flow in the section 9–16 does not change the direction at any time of the simulation period. In Fig. 6 are presented calculated and measured pressure differences between physical nodes 13 and 16. Since the pipeline 13–48 is not a physical pipeline, is modeled only form the numerical reasons and is very short, it can be assumed that pressures in nodes 13 and 48 are the same. Where pressure difference measured is the smallest, below

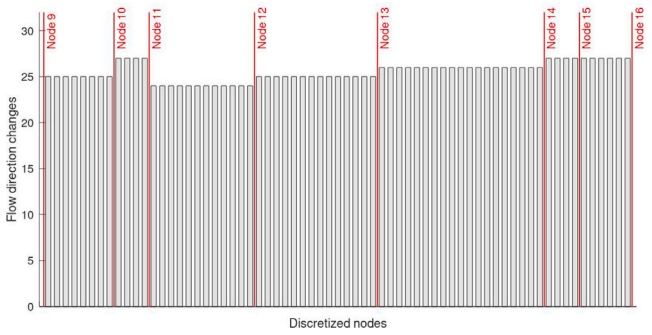

Fig. 5. Flow reversal occurrence in pipeline system section between physical nodes 9 and 16.

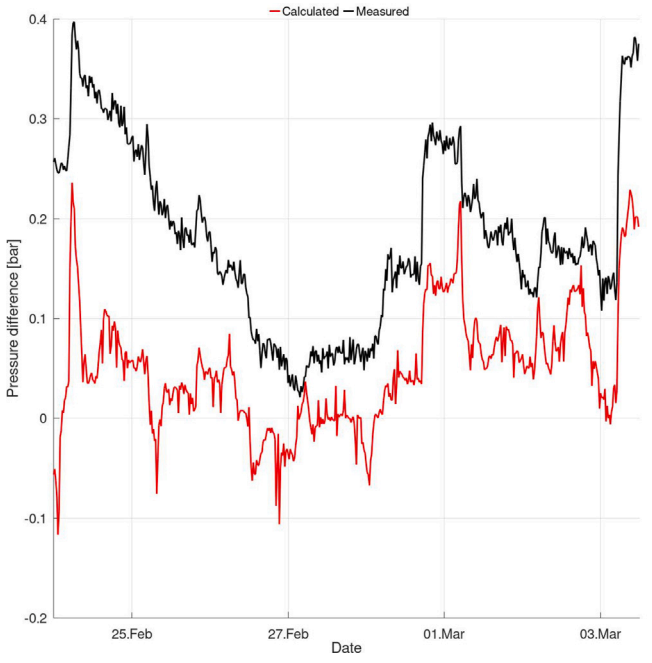

Fig. 6. Calculated and measured pressure difference between nodes 48 and 16.

0.1 bar, calculated pressure difference becomes negative meaning the flow direction changes and gas mixture flows from the node 16 to the node 13. Flow reversals occurs on the section 9–16 because it is a part of the loop, meaning offtake nodes in the loop can be supplied via two directions. The actual direction or a path by which an offtake node is supplied is defined by the hydraulic conditions in the loop, which are impacted by the amplitude and dynamics of the offtakes in the loop. In our case, the highest offtakes in the loop occurs in the nodes 9, which represents the supply of multiple consumers in two geographic regions (included in the model only as a measured offtake in a single node) and in the node 16, which also represents an origin for two branches with high demand. Offtakes from both nodes varies over time and since they are much higher than the other offtakes in the loop they also define hydraulic conditions in the loop and therefore the flow direction in the section 9–16.

Ethane concentration simulation results for θ values 0.6, 0.7, 0.8, 0.9, 1 (fully implicit scheme) and 0.51 are presented in Fig. 7. For $\theta < 0.51$ model is not convergent. Transfer of ethane concentration profile from the input node 1 to the output node 23 was measured at both

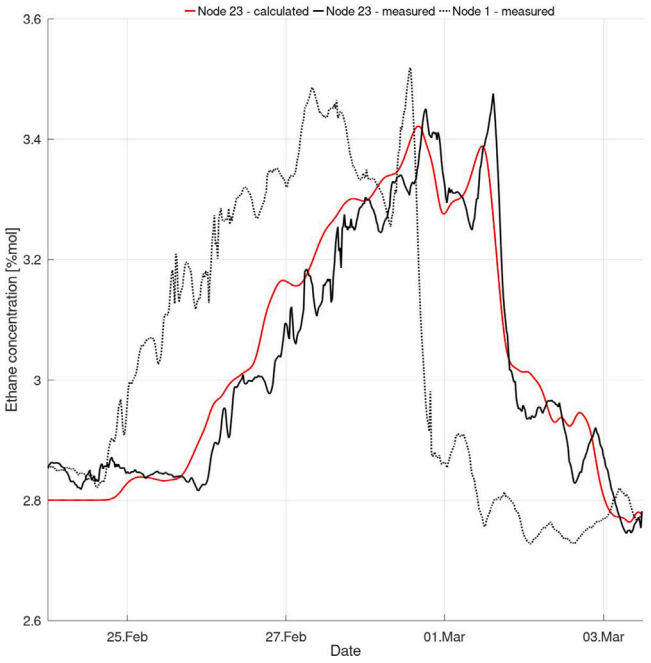

Fig. 7. Measured concentration of mass transfer of ethane component from the input (Node 1) to the output (Node 23) and comparison of measured output concentration to the calculated concentration of ethane.

nodes and measured output concentration profile is very similar to the measured input profile, but not exactly the same since gas was traveling from the input towards the output in two different routes. Simulated profile in the output node follows the measured profile yet all the finer details are lost in the simulated profile, which is to be expected due to the 1st order numerical scheme related distortions [30,32]. Reduced level of details of the solution is caused by the numerical diffusion. Loss of finer details is most visible at large θ values and with decreasing θ values the level of details is improving, but simulation results tends to oscillate more, which results in decreased convergence of the model.

Simulated ethane gradient started to increase sooner than the measured ethane gradient, regardless of the θ value used in the simulation. There could be two reasons for such behavior:

1. simulated flow velocity is higher than actual flow velocity (x-axis offset)
2. ethane concentration in the branch 16–23 is less diluted with lower ethane concentration gas mixture before the ethane profile peak and more diluted with higher ethane concentration gas mixture after the ethane concentration profile peak (y-axis offset) due to:
    a. smaller flows from pipeline 13–16 due to the smaller calculated pressure differences compared to the measured differences,
    b. absence of flow from pipeline 13–16 due to the reversed flow direction.

Flow velocity is affected considerably by the friction, which depends on the pipeline surface roughness. Since measurements for pipeline roughness for all the pipelines considered in the model are not available, the same pipeline roughness was considered in the simulation for all pipelines. Regarding the dilution of flow in 16–23, actual flow in 16–23 consists of flows from 40–16 and 9–16. Direction of simulated flow in 9–16 reverses multiple time meaning, that during reversed flow

Fig. 8. Comparison of calculated pressures with measured pressures for selected physical nodes.

period, 16–23 is supplied only from 40–16 and in that case flow is not diluted with the flow from 9–16 with the delayed ethane concentration profile which has lower ethane concentration when it reaches node 16 due to the longer transmission path. Lower calculated pressure difference between nodes 13 and 16, compared to the measured pressure difference lead to lower calculated flows than actual flows were, which contributes to the decreased impact of the composition of the gas from 9–16 to the composition in node 23. Flow and concentration profile from 40–16 has the dominant impact on the composition in node 23. This could explain why calculated profile is higher compared to the measured concentration profile.

The largest time delay between simulated and measured ethane profile is around 9 h. For comparison, time delay between simulated and measured ethane profile where flow reversal is not an issue as in [32], the largest time delay was ≈2 h. Effects of amplitude of the profile reduction are also visible in both ethane profile peaks, similar to simulation results in [30,32].

Although the simulation results for concentration tracking are not perfect, they are still sufficiently accurate for rough concentration tracking purposes, where great level of details is not necessary, especially considering all the unavoidable simplifications in the preparation of the input data and the model topology (in connection with the reverse flow).

Simulations of the pressures are, on the other hand, considerably more accurate, regardless of the value of θ parameter. Results are practically identical for all simulated θ values, as can be seen in Table 3, where the biggest differences between the measured pressure and the simulated pressure (pressure error) for each θ values and for each of the nodes, use for pressure validation are presented. Pressure errors for nodes 48, 26 and 35 are not included in the table, since the maximal pressure error was 0.4586 bar, 0.4254 bar and 0.5068 bar,

Table 3
Largest difference between measured and simulated pressure in bar at various values of θ parameter.

θ	Node 38	Node 8	Node 10	Node 25	Node 33
0.51	1.2198	0.5240	1.5931	0.2973	1.7006
0.6	1.2220	0.5232	1.5891	0.3027	1.7026
0.7	1.2270	0.5257	1.5839	0.3085	1.7062
0.8	1.2291	0.5329	1.5769	0.3139	1.7082
0.9	1.2310	0.5398	1.5706	0.3190	1.7099
1	1.2335	0.5465	1.5651	0.3238	1.7119

respectively. Those errors were the same for all simulated θ values. Discrepancy between simulated and measured pressures on the main transport route (nodes 48, 26, 25, 35) are negligible. Accuracy is reduced as we move away from the main transmission route (nodes 8, 33). Accuracy is decreased for node pressures in the section 9–13, where the flow reversal occurred the most often (nodes 10, 38). Flow reversals occurred not due to physical reasons but due to the inaccuracy of the model and consequently simulation results for this section are also the less accurate compared to nodes in other sections. As can be seen in Fig. 5 nodes 10 and 38 are in the section with the highest rate of flow reversal occurrence, flow in this section reversed 27 times. Flow in section 15–16 also reverses direction 27 times and since node 33 is at the end of the branch which originates in node 16, flow reversal also contributes to pressure calculation errors in node 33. Nevertheless the highest discrepancy between the simulated and measured pressures occurred in the node 33, and is around 1 bar. Node 33 is also the most distant from the main transmission pipeline route which means the accuracy of the simulation is the lowest in the end of the offtake branches — branches that are not connected to the other parts of the system (are not looped). Comparison between simulated and measured physical node pressures for the selected nodes is in Fig. 8. Since simulated pressure values are almost identical for all θ values results in Fig. 8 are from simulation with $\theta = 0.8$.

5. Conclusion

Aim of this paper was to assess accuracy of finite difference method with θ scheme with arbitrarily selected implicitness under assumption of binary gas mixture. Suitability of such modeling approach for simulating distributed and dynamic hydrogen injections in the natural gas system was analyzed. To obtain confident insights in suitability of the proposed model for use in actual operation applications, actual network topology with measured boundary conditions were used for model validation.

Based on the validation results the model is very suitable for the hydraulic calculation, where the very accurate distribution of the gas species is not of the utmost importance, although concentration accuracy can be increased by using finer spatial and temporal discretization steps. In this paper finer time step was not selected due to the fact that majority of the measured input data was sampled with the resolution of one hour and since details between the two consecutive measurements are not known, finer temporal discretization step would not contribute to the overall accuracy significantly.

Accuracy of the model could be further improved by using additional available measured data in the simulation, for example measured pressures in the pipeline junctions or in the offtake points. For the first case new type of the node with known pressure should be introduced. For the second case new type of node is not necessary, but due to the mathematical limitations offtake node cannot have known both pressure and flow. That can be mitigated by assuming offtake pressure in the non-physical node upstream of the offtake node which is only a short distance away from offtake physical node with known energy offtake. All the available measured data should be included in the simulation if possible.

Level of implicitness has impact only on the advection equation and only concentration tracking results are affected by the θ parameter, while the effect of the implicitness on the simulated pressure results is negligible. Although this is true for the case with low variability in concentration of the species, additional analyzes is required to assess the impact of the level of implicitness on the accuracy of simulated pressures in case of high concentration variability, which can occur in actual operating condition with hydrogen injection in case where hydrogen admissible levels would be high, e.g. 5% or more.

Binary mixture assumption decreased model complexity and enabled faster simulation. Although this assumption contributed to lower accuracy in concentration tracking, it still produced acceptable accuracy. Contribution of this assumption to the concentration tracking error depends on the variability of the concentrations of the components of the natural gas (without hydrogen). In case natural gas composition is stable, this assumption will not have as significant impact on accuracy as in case where natural gas composition is changing significantly. In case other methane based renewable and low carbon gases will be injected in the natural gas system in larger quantities, binary gas assumption should be assessed again.

The most valuable contribution of this research is the validation of the θ-scheme finite difference model with the binary gas mixture approach for simulation of the gas hydraulics in the complex network topologies which can be found in an actual gas systems in most countries. Results of the validation shows that proposed model and binary gas mixture approach can be used in real life applications regarding modeling and simulations of the gas system operation. Special attention was given to the description of the modeling approach from the perspective of both the preparation of the input data and the topology modeling. Limitations of the model and mitigations to those limitations can be helpful for readers when building their own models of complex gas systems. Occurrence and impact of the non-physical flow direction reversal was explained in the paper which would also be helpful for the readers so they could pay special attention to this phenomena when building their own models for gas species concentration purposes.

Study presented in this paper can be further upgraded assuming different measured input data (operational cases) are available. Since measured data of only single occurrence of the gas species change was available for the model validation conducted in this study, model should also be validated in case with more dynamic gas species concentration variations. Since the proposed model is intended to be used for modeling coupled gas in electrical power systems, it should be validated with operational cases that would more closely resemble expected operational conditions of such coupled energy system-simulation of multiple spatially distributed and dynamic hydrogen (or other species of a gas mix) injections leading to hydrogen concentrations in wider range of allowable concentrations.

Declaration of competing interest

The authors declare that they have no known competing financial interests or personal relationships that could have appeared to influence the work reported in this paper.

Appendix

See Eqs. (25)–(30) in Box I.

$$\frac{p_i^{n+1}-p_i^n}{\Delta t}+\frac{K_1\left(1+\frac{\left(p_i^{n+1}+p_i^n\right)}{\left(y_i^{n+1}+y_i^n\right)\left(p_{c,H2}-p_{c,NG}\right)+2p_{c,NG}}\left(0.257-0.533\frac{\left(y_i^{n+1}+y_i^n\right)\left(T_{c,H2}-T_{c,NG}\right)+2T_{c,NG}}{2T}\right)\right)\left((1-\theta)\left(\dot{m}_{i+1}^n-\dot{m}_{i-1}^n\right)+\theta\left(\dot{m}_{i+1}^{n+1}-\dot{m}_{i-1}^{n+1}\right)\right)}{\Delta x\left(\left(y_i^{n+1}+y_i^n\right)\left(M_{H2}-M_{NG}\right)+2M_{NG}\right)}=0 \tag{25}$$

$$\frac{\dot{m}_i^{n+1}-\dot{m}_i^n}{A\Delta t}+\frac{(1-\theta)\left(p_{i+1}^n-p_{i-1}^n\right)+\theta\left(p_{i+1}^{n+1}-p_{i-1}^{n+1}\right)}{2\Delta x}+\frac{K_2\left(1+\frac{\left(p_i^{n+1}+p_i^n\right)}{\left(y_i^{n+1}+y_i^n\right)\left(p_{c,H2}-p_{c,NG}\right)+2p_{c,NG}}\left(0.257-0.533\frac{\left(y_i^{n+1}+y_i^n\right)\left(T_{c,H2}-T_{c,NG}\right)+2T_{c,NG}}{2T}\right)\right)\left(\dot{m}_i^{n+1}+\dot{m}_i^n\right)\left|\dot{m}_i^{n+1}+\dot{m}_i^n\right|}{\left(p_i^{n+1}+p_i^n\right)\left(\left(y_i^{n+1}+y_i^n\right)\left(M_{H2}-M_{NG}\right)+2M_{NG}\right)}=0 \tag{26}$$

$$\frac{y_i^{n+1}-y_i^n}{\Delta t}+\frac{K_1\left(1+\frac{\left(p_i^{n+1}+p_i^n\right)}{\left(y_i^{n+1}+y_i^n\right)\left(p_{c,H2}-p_{c,NG}\right)+2p_{c,NG}}\left(0.257-0.533\frac{\left(y_i^{n+1}+y_i^n\right)\left(T_{c,H2}-T_{c,NG}\right)+2T_{c,NG}}{2T}\right)\right)\left(\dot{m}_i^{n+1}+\dot{m}_i^n\right)\left((1-\theta)\left(y_{i+1}^n-y_{i-1}^n\right)+\theta\left(y_{i+1}^{n+1}-y_{i-1}^{n+1}\right)\right)}{\Delta x\left(p_i^{n+1}+p_i^n\right)\left(\left(y_i^{n+1}+y_i^n\right)\left(M_{H2}-M_{NG}\right)+2M_{NG}\right)}=0 \tag{27}$$

$$\frac{p_i^{n+1}-p_i^n}{\Delta t}+\frac{K_1\left(1+\frac{\left(p_i^{n+1}+p_i^n\right)}{\left(y_i^{n+1}+y_i^n\right)\left(p_{c,H2}-p_{c,NG}\right)+2p_{c,NG}}\left(0.257-0.533\frac{\left(y_i^{n+1}+y_i^n\right)\left(T_{c,H2}-T_{c,NG}\right)+2T_{c,NG}}{2T}\right)\right)\left((1-\theta)\left(3\dot{m}_i^n-4\dot{m}_{i-1}^n+\dot{m}_{i-2}^n\right)+\theta\left(3\dot{m}_i^{n+1}-4\dot{m}_{i-1}^{n+1}+\dot{m}_{i-2}^{n+1}\right)\right)}{\Delta x\left(\left(y_i^{n+1}+y_i^n\right)\left(M_{H2}-M_{NG}\right)+2M_{NG}\right)}=0 \tag{28}$$

$$\frac{\dot{m}_i^{n+1}-\dot{m}_i^n}{A\Delta t}+\frac{(1-\theta)\left(3p_i^n-4p_{t-1}^n+p_{t-2}^n\right)+\theta\left(3p_t^{n+1}-4p_{t-1}^{n+1}+p_{t-2}^{n+1}\right)}{2\Delta x}+\frac{K_2\left(1+\frac{\left(p_i^{n+1}+p_i^n\right)}{\left(y_i^{n+1}+y_i^n\right)\left(p_{c,H2}-p_{c,NG}\right)+2p_{c,NG}}\left(0.257-0.533\frac{\left(y_i^{n+1}+y_i^n\right)\left(T_{c,H2}-T_{c,NG}\right)+2T_{c,NG}}{2T}\right)\right)\left(\dot{m}_i^{n+1}+\dot{m}_i^n\right)\left|\dot{m}_i^{n+1}+\dot{m}_i^n\right|}{\left(p_i^{n+1}+p_i^n\right)\left(\left(y_i^{n+1}+y_i^n\right)\left(M_{H2}-M_{NG}\right)+2M_{NG}\right)}=0 \tag{29}$$

$$\frac{y_i^{n+1}-y_i^n}{\Delta t}+\frac{K_1\left(1+\frac{\left(p_i^{n+1}+p_i^n\right)}{\left(y_i^{n+1}+y_i^n\right)\left(p_{c,H2}-p_{c,NG}\right)+2p_{c,NG}}\left(0.257-0.533\frac{\left(y_i^{n+1}+y_i^n\right)\left(T_{c,H2}-T_{c,NG}\right)+2T_{c,NG}}{2T}\right)\right)\left(\dot{m}_i^{n+1}+\dot{m}_i^n\right)\left((1-\theta)\left(3y_i^n-4y_{i-1}^n+y_{i-2}^n\right)+\theta\left(3y_i^{n+1}-4y_{i-1}^{n+1}+y_{l-2}^{n+1}\right)\right)}{\Delta x\left(p_i^{n+1}+p_i^n\right)\left(\left(y_i^{n+1}+y_i^n\right)\left(M_{H2}-M_{NG}\right)+2M_{NG}\right)}=0 \tag{30}$$

Box I.

References

[1] Weitzel M, Vandyck T, Rey Los Santos L, Tamba M, Temursho U, Wojtowicz K. A comprehensive socio-economic assessment of EU climate policy pathways. Ecol Econom 2023;204:107660. http://dx.doi.org/10.1016/j.ecolecon.2022.107660.

[2] Kuzemko C, Blondeel M, Dupont C, Brisbois MC. Russia's war on Ukraine, European energy policy responses & implications for sustainable transformations. Energy Res Soc Sci 2022;93:102842. http://dx.doi.org/10.1016/j.erss.2022.102842.

[3] Erdener BC, Sergi B, Guerra OJ, Lazaro Chueca A, Pambour K, Brancucci C, Hodge B-M. A review of technical and regulatory limits for hydrogen blending in natural gas pipelines. Int J Hydrogen Energy 2023;48(14):5595–617. http://dx.doi.org/10.1016/j.ijhydene.2022.10.254.

[4] Pluvinage G. Mechanical properties of a wide range of pipe steels under influence of pure hydrogen or hydrogen blended with natural gas. Int J Press Vessels Pip 2021;190:104293. http://dx.doi.org/10.1016/j.ijpvp.2020.104293.

[5] Galyas AB, Kis L, Tihanyi L, Szunyog I, Vadaszi M, Koncz A. Effect of hydrogen blending on the energy capacity of natural gas transmission networks. Int J Hydrogen Energy 2023;48(39):14795–807. http://dx.doi.org/10.1016/j.ijhydene.2022.12.198.

[6] Kuczyński S, Łaciak M, Olijnyk A, Szurlej A, Włodek T. Thermodynamic and technical issues of hydrogen and methane-hydrogen mixtures pipeline transmission. Energies 2019;12(3). http://dx.doi.org/10.3390/en12030569.

[7] Thawani B, Hazael R, Critchley R. Assessing the pressure losses during hydrogen transport in the current natural gas infrastructure using numerical modelling. Int J Hydrogen Energy 2023;48(88):34463–75. http://dx.doi.org/10.1016/j.ijhydene.2023.05.208.

[8] Le TT, Sharma P, Bora BJ, Tran VD, Truong TH, Le HC, Nguyen PQP. Fueling the future: A comprehensive review of hydrogen energy systems and their challenges. Int J Hydrogen Energy 2023. http://dx.doi.org/10.1016/j.ijhydene.2023.08.044.

[9] Guan D, Wang B, Zhang J, Shi R, Jiao K, Li L, Wang Y, Xie B, Zhang Q, Yu J, Zhu Y, Shao Z, Ni M. Hydrogen society: from present to future. Energy Environ Sci 2023. http://dx.doi.org/10.1039/D3EE02695G.

[10] Elberry AM, Thakur J, Santasalo-Aarnio A, Larmi M. Large-scale compressed hydrogen storage as part of renewable electricity storage systems. Int J Hydrogen Energy 2021;46(29):15671–90. http://dx.doi.org/10.1016/j.ijhydene.2021.02.080.

[11] Muthukumar P, Kumar A, Afzal M, Bhogilla S, Sharma P, Parida A, Jana S, Kumar EA, Pai RK, Jain I. Review on large-scale hydrogen storage systems for better sustainability. Int J Hydrogen Energy 2023;48(85):33223–59. http://dx.doi.org/10.1016/j.ijhydene.2023.04.304.

[12] Ishaq H, Dincer I, Crawford C. A review on hydrogen production and utilization: Challenges and opportunities. Int J Hydrogen Energy 2022;47(62):26238–64. http://dx.doi.org/10.1016/j.ijhydene.2021.11.149, SI: Progress in Hydrogen Production, Storage and Distribution (Ahmadi).

[13] Parkinson B, Balcombe P, Speirs JF, Hawkes AD, Hellgardt K. Levelized cost of CO2 mitigation from hydrogen production routes. Energy Environ Sci 2019;12:19–40. http://dx.doi.org/10.1039/C8EE02079E.

[14] Reigstad GA, Roussanaly S, Straus J, Anantharaman R, de Kler R, Akhurst M, Sunny N, Goldthorpe W, Avignon L, Pearce J, Flamme S, Guidati G, Panos E, Bauer C. Moving toward the low-carbon hydrogen economy: Experiences and key learnings from national case studies. Adv Appl Energy 2022;8:100108. http://dx.doi.org/10.1016/j.adapen.2022.100108.

[15] Zhang Z, Saedi I, Mhanna S, Wu K, Mancarella P. Modelling of gas network transient flows with multiple hydrogen injections and gas composition tracking. Int J Hydrogen Energy 2022;47(4):2220–33. http://dx.doi.org/10.1016/j.ijhydene.2021.10.165.

[16] Sharma P, Sivaramakrishnaiah M, Deepanraj B, Saravanan R, Reddy MV. A novel optimization approach for biohydrogen production using algal biomass. Int J Hydrogen Energy 2022. http://dx.doi.org/10.1016/j.ijhydene.2022.09.274.

[17] Grigoriev S, Fateev V, Bessarabov D, Millet P. Current status, research trends, and challenges in water electrolysis science and technology. Int J Hydrogen Energy 2020;45(49):26036–58. http://dx.doi.org/10.1016/j.ijhydene.2020.03.109, Progress in Hydrogen Production and Utilization.

[18] Danieli P, Lazzaretto A, Al-Zaili J, Sayma A, Masi M, Carraro G. The potential of the natural gas grid to accommodate hydrogen as an energy vector in transition towards a fully renewable energy system. Appl Energy 2022;313:118843. http://dx.doi.org/10.1016/j.apenergy.2022.118843.

[19] Vaziri Rad MA, Kasaeian A, Niu X, Zhang K, Mahian O. Excess electricity problem in off-grid hybrid renewable energy systems: A comprehensive review from challenges to prevalent solutions. Renew Energy 2023;212:538–60. http://dx.doi.org/10.1016/j.renene.2023.05.073.

[20] Impram S, Varbak Nese S, Oral B. Challenges of renewable energy penetration on power system flexibility: A survey. Energy Strategy Rev 2020;31:100539. http://dx.doi.org/10.1016/j.esr.2020.100539.

[21] Wang Y, Qiu J, Tao Y. Robust energy systems scheduling considering uncertainties and demand side emission impacts. Energy 2022;239:122317. http://dx.doi.org/10.1016/j.energy.2021.122317.

[22] Xiao H, Long F, Zeng L, Zhao W, Wang J, Li Y. Optimal scheduling of regional integrated energy system considering multiple uncertainties and integrated demand response. Electr Power Syst Res 2023;217:109169. http://dx.doi.org/10.1016/j.epsr.2023.109169.

[23] Wang C, Zhou D, Xiao W, Shui C, Ma T, Chen P, Hao J, Yan J. Research on the dynamic characteristics of natural gas pipeline network with hydrogen injection considering line-pack influence. Int J Hydrogen Energy 2023. http://dx.doi.org/10.1016/j.ijhydene.2023.03.298.

[24] Peterson P. A method for predicting and minimizing numerical diffusion. Numer Heat Transfer B 1992;21(3):343–66. http://dx.doi.org/10.1080/10407799208944909, arXiv:https://www.tandfonline.com/doi/pdf/10.1080/10407799208944909.

[25] Ferreira V, de Queiroz R, Lima G, Cuenca R, Oishi C, Azevedo J, McKee S. A bounded upwinding scheme for computing convection-dominated transport problems. Comput & Fluids 2012;57:208–24. http://dx.doi.org/10.1016/j.compfluid.2011.12.021.

[26] Østerby O. Five ways of reducing the Crank-Nicolson oscillations. BIT Numer Math 2003;(43):811–22. http://dx.doi.org/10.1023/B:BITN.0000009942.00540.94.

[27] Gnedin NY, Semenov VA, Kravtsov AV. Enforcing the Courant–Friedrichs–Lewy condition in explicitly conservative local time stepping schemes. J Comput Phys 2018;359:93–105. http://dx.doi.org/10.1016/j.jcp.2018.01.008.

[28] Helgaker JF, Oosterkamp A, Langelandsvik LI, Ytrehus T. Validation of 1D flow model for high pressure offshore natural gas pipelines. J Nat Gas Sci Eng 2014;16:44–56. http://dx.doi.org/10.1016/j.jngse.2013.11.001.

[29] Helgaker JF, Ytrehus T. Coupling between continuity/momentum and energy equation in 1D gas flow. Energy Procedia 2012;26:82–9. http://dx.doi.org/10.1016/j.egypro.2012.06.013, 2nd Trondheim Gas Technology Conference.

[30] Dancker J, Wolter M. A coupled transient gas flow calculation with a simultaneous calorific-value-gradient improved hydrogen tracking. Appl Energy 2022;316:118967. http://dx.doi.org/10.1016/j.apenergy.2022.118967.

[31] Chaczykowski M, Zarodkiewicz P. Simulation of natural gas quality distribution for pipeline systems. Energy 2017;134:681–98. http://dx.doi.org/10.1016/j.energy.2017.06.020.

[32] Chaczykowski M, Sund F, Zarodkiewicz P, Hope SM. Gas composition tracking in transient pipeline flow. J Nat Gas Sci Eng 2018;55:321–30. http://dx.doi.org/10.1016/j.jngse.2018.03.014.

[33] Fan D, Gong J, Zhang S, Shi G, Kang Q, Xiao Y, Wu C. A transient composition tracking method for natural gas pipe networks. Energy 2021;215:119131. http://dx.doi.org/10.1016/j.energy.2020.119131.

[34] Bermúdez A, Shabani M. Numerical simulation of gas composition tracking in a gas transportation network. Energy 2022;247:123459. http://dx.doi.org/10.1016/j.energy.2022.123459.

[35] Bermúdez A, López X, Vázquez-Cendón ME. Reprint of: Finite volume methods for multi-component Euler equations with source terms. Comput & Fluids 2018;169:40–61. http://dx.doi.org/10.1016/j.compfluid.2018.03.057, Recent progress in nonlinear numerical methods for time-dependent flow & transport problems.

[36] Uilhoorn F. Dynamic behaviour of non-isothermal compressible natural gases mixed with hydrogen in pipelines. Int J Hydrogen Energy 2009;34(16):6722–9. http://dx.doi.org/10.1016/j.ijhydene.2009.06.062, 4th Dubrovnik Conference.

[37] Pambour KA, Bolado-Lavin R, Dijkema GP. An integrated transient model for simulating the operation of natural gas transport systems. J Nat Gas Sci Eng 2016;28:672–90. http://dx.doi.org/10.1016/j.jngse.2015.11.036.

[38] Ke S, Ti H. Transient analysis of isothermal gas flow in pipeline network. Chem Eng J 2000;76(2):169–77. http://dx.doi.org/10.1016/S1385-8947(99)00122-9.

[39] Elaoud S, Hafsi Z, Hadj-Taieb L. Numerical modelling of hydrogen-natural gas mixtures flows in looped networks. J Pet Sci Eng 2017;159:532–41. http://dx.doi.org/10.1016/j.petrol.2017.09.063.

[40] Su H, Zio E, Zhang Z-J, Xiong C-Z, Dai Q-S, Wu Q-W, Zhang J-J. Development of an integrated dynamic model for supply security and resilience analysis of natural gas pipeline network systems. Pet Sci 2022;19(2):761–73. http://dx.doi.org/10.1016/j.petsci.2021.10.002.

[41] Alamian R, Behbahani-Nejad M, Ghanbarzadeh A. A state space model for transient flow simulation in natural gas pipelines. J Nat Gas Sci Eng 2012;9:51–9. http://dx.doi.org/10.1016/j.jngse.2012.05.013.

[42] Hafsi Z, Elaoud S, Mishra M. A computational modelling of natural gas flow in looped network: Effect of upstream hydrogen injection on the structural integrity of gas pipelines. J Nat Gas Sci Eng 2019;64:107–17. http://dx.doi.org/10.1016/j.jngse.2019.01.021.

[43] Elaoud S, Hadj-Taïeb E. Transient flow in pipelines of high-pressure hydrogen–natural gas mixtures. Int J Hydrogen Energy 2008;33(18):4824–32. http://dx.doi.org/10.1016/j.ijhydene.2008.06.032.

[44] Chaczykowski M. Transient flow in natural gas pipeline – The effect of pipeline thermal model. Appl Math Model 2010;34(4):1051–67. http://dx.doi.org/10.1016/j.apm.2009.07.017.

[45] Chaczykowski M. Sensitivity of pipeline gas flow model to the selection of the equation of state. Chem Eng Res Des 2009;87(12):1596–603. http://dx.doi.org/10.1016/j.cherd.2009.06.008.

[46] Benner P, Grundel S, Himpe C, Huck C, Streubel T, Tischendorf C. Gas network benchmark models. In: Campbell S, Ilchmann A, Mehrmann V, Reis T, editors. Applications of differential-algebraic equations: Examples and benchmarks. Cham: Springer International Publishing; 2019, p. 171–97. http://dx.doi.org/10.1007/11221_2018_5.

[47] Faragó I. Convergence and stability constant of the theta-method. Appl Math 2013;42–51.

[48] Liang H, Liu M, Lv W. Stability of θ-schemes in the numerical solution of a partial differential equation with piecewise continuous arguments. Appl Math Lett 2010;23(2):198–206. http://dx.doi.org/10.1016/j.aml.2009.09.012.

[49] Chapra S, Canale R. Numerical methods for engineers, Vol. 33. 7th ed.. McGraw-Hill Science/Engineering/Math; 2015, no. 3.

[50] Freitas CJ. The issue of numerical uncertainty. Appl Math Model 2002;26(2):237–48. http://dx.doi.org/10.1016/S0307-904X(01)00058-0.